

Thermal and mechanical properties of SEBS-g-MA based inorganic composite materials

Sonia Zulfiqar · Zahoor Ahmad · Muhammad Ishaq ·
Shaikat Saeed · Muhammad Ilyas Sarwar

Received: 12 March 2005 / Accepted: 6 January 2006 / Published online: 9 November 2006
© Springer Science+Business Media, LLC 2006

Abstract Organic-inorganic hybrids based on a tri-block copolymer [polystyrene-*b*-poly (ethylene-*ran*-butylene)-*b*-polystyrene-*g*-maleic anhydride] (SEBS-*g*-MA) with silica and clay were prepared using sol-gel and solution intercalation methods respectively. Reinforcement in the first system was achieved by the in-situ hydrolysis/condensation of tetraethoxysilane in the copolymer matrix yielding hybrid materials. The interaction between organic and inorganic phases was developed through a coupling agent. In another system, copolymer was reinforced by organoclay and compatibility between copolymer and hydrophilic montmorillonite was achieved by intercalation of clay with dodecylamine which increased the organophilicity of the clay. Thin transparent films of these hybrids materials were characterized for their mechanical, thermal and thermomechanical behavior. The tensile strength of hybrids improved relative to the pure copolymer in all the systems. Dynamic mechanical thermal analysis carried out gave α -relaxation temperature associated with glass transition temperature (T_g). The results indicate a shift in T_g values with the addition of silica in the matrix, which suggests an increased interfacial interaction between organic and

inorganic phases while this effect is less pronounced in polymer-clay system. Thermal decomposition temperatures of the hybrids were found in the range of 450–500 °C. The weights of the residues left at 700 °C were nearly proportional to the inorganic contents in the original hybrids.

Introduction

Hybrid organic-inorganic materials typically exhibit properties superior to those of their individual components. To optimize the performance properties of these materials, the dispersion of inorganic phase in the organic matrix at nano- or micro-meter level is desirable. One successful approach to achieve such nanocomposites is the in-situ polymerization of metal alkoxides in organic materials via the sol-gel process [1–8], a convenient and flexible route for producing hybrid materials at low temperature. The composition and homogeneity of such hybrid materials can be controlled at molecular level. The incorporation of organic polymers particularly elastomers impart flexibility to the inorganic glasses while the introduction of the inorganic component can improve the properties of organic polymers. These materials are useful in electrical, structural or coating applications. Inorganic component, especially silica has been generated by the hydrolysis and condensation of organic precursor; such as tetraethoxysilane (TEOS) in many polymer systems [9–12] due to its relatively slow and controllable rate of reaction. For multicomponent hybrid materials, metal alkoxides based on aluminum,

S. Zulfiqar · M. Ishaq · M. I. Sarwar (✉)
Department of Chemistry, Quaid-i-Azam University,
Islamabad 45320, Pakistan
e-mail: ilyassarwar@hotmail.com

Z. Ahmad
Department of Chemistry, Faculty of Science, Kuwait
University, P.O. Box: 5969, Safat 13060, Kuwait

S. Saeed
Department of Chemical and Materials Engineering,
PIEAS, Islamabad 45320, Pakistan

titanium and zirconium (all have relatively fast hydrolysis rates) can be employed. The homogenous product can be obtained with almost any composition with some modification of the reaction procedure. Mark and coworkers [13] have infused poly(dimethylsiloxane) films with TEOS and precipitated silica particles by means of sol-gel process. Wilkes and colleagues [14, 15] reported hybrids of silica with hydroxy-terminated polydimethylsiloxane and polytetramethyleneoxide. Hybrids based on zirconia and titania with same polymer matrices have also been produced by the same workers [16, 17]. The introduction of titania or zirconia into the hybrid system improves the modulus and stress at break of the hybrids. Hybrids from high performance polymers such as polyamides, polyimides [8, 18–26] have been reported by the present authors. Another approach to the synthesis of nanocomposites is the dispersion or break down of inorganic clay minerals consisting of layered silicates into nanoscale building blocks in the polymer materials. In recent years due to the unique combination of advantageous properties of each component, there has been considerable interest in the formation of polymer–clay nanocomposites. Through intercalation a large number of polymer–clay nanocomposites were reported, such as hybrids containing single silicate layer uniformly dispersed in nylon matrix [27]. Tensile strength, impact resistance, thermal and radiological properties of the nylon were improved upon 4–7 wt.% loading of clay while the water absorption reduced considerably for the nanocomposites. Significant increase in the heat distortion temperature has been reported which makes nylon more useful in high temperature applications. Organically modified mica type silicate dispersed in epoxy resin [28] showed improvement in mechanical properties and reduction in permeability as compared to the unfilled polymers. This reduction in permeability was due to dispersed silicate layers with a large aspect ratio in the matrix. Many other epoxy based clay nanocomposites have been reported recently [29–31]. Some other organic-inorganic hybrids with clays included poly(methylmethacrylate) [32], polystyrene [33–36], polypropylene [34, 37–39], polyester [40], poly(etherimide) [41], polyacrylate [42] and polyimides matrices [43, 44]. These all show potentially hybrid properties synergistically derived from both the clay and polymer [45–47]. In the present study, SEBS-g-MA was reinforced with silica as well as with layered silicates. In this regard, copolymer chains were reinforced with either silica network using TEOS as precursor through sol-gel process or by dispersing organophilic montmorillonite in the matrix through solution intercalation technique using THF as a

solvent. Thin hybrid films were cast by evaporating the solvent. These films were subjected to mechanical, thermal and dynamic mechanical thermal analyses.

Experimental section

Materials

SEBS-g-MA with 1.8-wt.% grafted maleic anhydride contents supplied by Aldrich has molecular weight 20,000. Tetraethoxysilane (TEOS) (99%), triethylamine (99%), anhydrous calcium oxide (99.9%), montmorillonite K-10 and dodecylamine (98%) were obtained from Aldrich and used as such. Hydrochloric acid (99%), benzophenone (99%), sodium metal (large pieces in kerosene) supplied by Fluka and aminophenyl trimethoxysilane (APTMS) (97%) provided by Hüls were used as received. Tetrahydrofuran (THF) provided by Merck was first distilled at constant boiling temperature, followed by the addition of calcium oxide and left overnight. After filtration, it was refluxed using sodium wire with benzophenone as indicator. The deep blue color of the solution confirmed the drying of THF. Dried THF was then collected by distillation and used as solvent.

Montmorillonite (cation exchange capacity of 119 meq/100 g) was intercalated using 8.82 g of dodecylamine and 4.8 ml of concentrated hydrochloric acid in 100 ml of distilled water. This solution was heated at 80 °C. In a separate beaker, 20 g of Na-montmorillonite was dispersed in distilled water at 80 °C. This dispersed montmorillonite was added to the solution of ammonium salt of dodecylamine and the resulting mixture was vigorously stirred for 3 h at 60 °C and white precipitates were isolated by filtration. These precipitates were washed with 400 ml of hot water and then filtered. This process was repeated thrice to remove the residue of ammonium salt of dodecylamine. The final product obtained by filtration was dried in vacuum oven at 60 °C for 24 h. The intercalated clay powder thus obtained was employed for preparing the hybrid materials.

SEBS-g-MA and silica hybrids

A stock solution of copolymer was prepared by dissolving 10.0 g of SEBS-g-MA in 70.0 g of dried THF (as a solvent) with constant stirring for 24 h. Triethylamine was added as catalyst for the sol-gel process. Hybrids were prepared by mixing various concentrations of TEOS with an appropriate amount of copolymer solution. After complete mixing, measured

amount of water was added to the reaction mixture to carry out the hydrolysis and condensation of TEOS with further stirring and heating for 6 h at 60 °C. Interaction between the two phases was developed through coupling agent in the related second system. For this purpose, to the fresh stock solution of SEBS-g-MA, 1.8-wt.% of coupling agent (APT MOS) was mixed with constant stirring for 6 h. Then different amounts of TEOS were mixed with copolymer solutions. The hydrolysis and condensation of APT MOS and TEOS upon the addition of stoichiometric amount of water was carried out for 6 h at 60 °C. Silica concentrations varied from 2.5–30 wt.% in the matrix. Films of thickness (0.25–0.30 mm) were cast by the solvent evaporation technique. These hybrid films were finally dried at 80 °C under vacuum for 72 h to a constant weight.

SEBS-g-MA and clay hybrids

Composites with different clay concentrations were prepared by mixing different amounts of intercalated clay to the copolymer solution. Hybrid films of uniform and controlled thickness were obtained by solvent elution technique. Films were further dried at 80 °C under vacuum for 72 h to a constant weight.

Characterization

Tensile properties of the hybrid films with dimensions (ca. 14×5.0 – 7.4×0.20 – 0.39 mm) were measured according to DIN procedure 53455 having a crosshead speed of 0.1 cm min^{-1} at 25 °C using Testometric Universal Testing Machine M350/500 at room temperature and an average value obtained from 5–7 different measurements in each case has been reported. The dynamic mechanical thermal analysis was performed on the hybrid materials in the temperature range 40–120 °C using a frequency of 5 Hz with DMA Q800 in bending mode. TGA on the hybrid samples was

performed with TGA-7 Thermogravimetric Analyzer by using 1–5 mg of the sample in Al_2O_3 crucible heated from 100–700 °C at a heating rate of 10 °C min^{-1} under nitrogen atmosphere with a gas flow rate of 50 ml min^{-1} .

Results and discussion

Thermoplastic elastomer SEBS-g-MA reinforced with inorganic fillers such as silica, and layered silicates using the sol-gel and solution intercalation techniques have been studied for the following properties.

Mechanical properties of SEBS-g-MA hybrids

The stress-strain data for the copolymer–silica composite films are given in Table 1 and Fig. 1. The results show increase in the tensile strength of the hybrid materials relative to the pure copolymer. The initial moduli of the samples were calculated from the initial slopes of the stress-strain curves. The pure copolymer had a value of tensile modulus 55 MPa that increased to a maximum value 92 MPa with 2.5-wt.% silica, beyond this it decreased. The ultimate stress at break for the pure copolymer is 15 MPa that increases up to 29 MPa with 7.5-wt.% of silica and then decreases with further addition of silica. The elongation at rupture increases up to 5.0-wt.% silica contents and then shows a decreasing trend with higher amount of silica. These results show improvement in the tensile strength of hybrid materials as compared to the pure copolymer.

The overall tensile behavior of hybrid materials show initial high modulus due to entanglement of polymeric chains and then a region of low modulus in which the chains slip over each other and increase in stress values is small. Then increase in the mechanical properties may be due to alignment of the chains that resist applied load. It also suggests that silica when incorporated in small amounts arranged itself in the

Table 1 Mechanical properties of SEBS-g-MA-silica hybrid materials

Sample No.	Silica Contents(%)	Maximum Stress (MPa) ± 3.00	Maximum Strain ± 0.02	Initial Modulus (MPa) ± 0.02	Toughness (MPa) ± 5.00
1	0.0	14.93	12.39	55	79.35
2	2.5	24.11	13.46	92	118.32
3	5.0	26.12	14.39	76	137.49
4	7.5	29.10	13.97	69	153.45
5	10.0	25.43	13.89	67	129.26
6	12.5	25.01	13.73	63	125.69
7	15.0	22.56	12.85	61	111.60
8	20.0	18.54	12.22	59	92.22
9	25.0	15.74	12.09	55	84.30
10	30.0	15.04	12.07	31	77.53

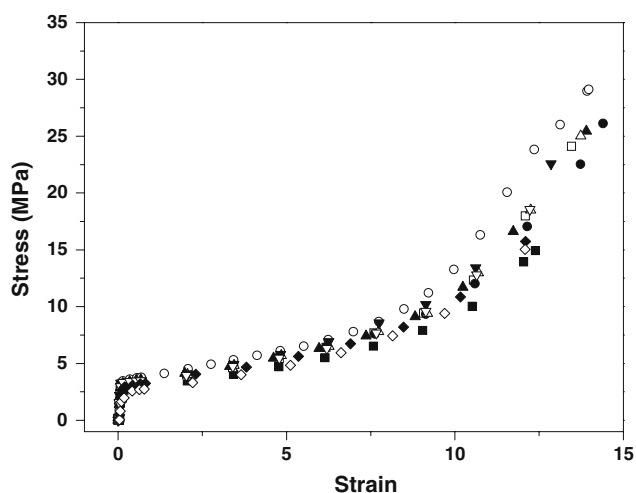


Fig. 1 Stress-strain curves of SEBS-g-MA-silica hybrids without interphase bonding; silica% in matrix: 0 (■), 2.5 (□), 5.0 (●), 7.5 (○), 10.0 (▲), 12.5(△), 15.0 (▼), 20.0 (▽), 25.0 (◆), 30.0 (◇)

form of very small particles, with sizes increasing at the higher silica contents. The inorganic particle size increased, possibly by forming clusters. This may lead the distribution of the inorganic phase in the matrix less uniform, thus increasing the number of defects or flaws in the hybrid materials, which can cause brittleness. This results in poor interfacial interactions between the two disparate phases. Toughness of these materials was measured by integrating the area under stress-strain curves up to their maximum extension, which corresponds to the energy or work required for rupture. The values initially increase and then decrease with high percentage of silica. The optimum value obtained for 7.5-wt.% silica is 153 MPa relative to the pure copolymer (79 MPa).

The variation of tensile strength with silica contents for the compatibilized SEBS-g-MA-silica system is shown in Table 2 and Fig. 2. Tensile modulus initially shows slightly lower values than pure copolymer that increase with the addition of inorganic contents. The

maximum increase in the ultimate stress is noted with 2.5-wt.% silica, which then decreases gradually with silica contents greater than 30-wt.%. It is evident that there is an increase in the tensile strength as compared with that of the pure copolymer. There is a decrease in strain value relative to pure copolymer with increase in the silica contents.

Toughness increases with increase in the inorganic contents up to 2.5-wt.%. However, toughness of compatibilized system is lower than the corresponding un-compatibilized system. In case of copolymer–silica system having no interphase bonding maximum toughness obtained is for 7.5-wt.% silica (153 MPa) while in compatibilized system toughness increased to 101 MPa for 2.5-wt.% silica. Unfortunately, toughness and mechanical properties of the un-compatibilized system have improved relative to the compatibilized system. This trend may be explained in terms of the plasticization effect of coupling agent that results in the reduction of the mechanical properties of this system as compared to the un-compatibilized system. Actually the purpose of the coupling agent is to create a chemical linkage between the matrix and the filler (silica). The amine end of the coupling agent can react with anhydride group in polymer chain and alkoxy group can condense with TEOS thus creating interaction between the disparate phases. The IR data indicates that some anhydride groups have changed into free acid and the reaction of the free acid with amino group of the coupling agent only takes place at higher temperature. So, most of the coupling agent may not be able to link with polymer chains and acts as plasticizer, thereby, deteriorating the mechanical properties. However, the relative increase in tensile strength of compatibilized system due to the introduction of silica into copolymer is much larger than those obtained with the un-compatibilized system. This may be due to the large number of bonding sites available in the compatibilized system, which became chemically

Table 2 Mechanical properties of SEBS-g-MA-silica hybrid materials compatibilized using APTMOS

Sample No.	Silica Contents (%)	Maximum Stress (MPa) \pm 3.00	Maximum Strain \pm 0.02	Initial Modulus (MPa) \pm 0.02	Toughness (MPa) \pm 5.00
1	0.0	14.93	12.39	55	79.35
2	2.5	23.16	11.41	48	101.76
3	5.0	21.91	11.14	50	93.83
4	7.5	21.77	10.68	52	86.69
5	10.0	20.28	10.41	54	86.02
6	12.5	20.02	9.69	55	72.17
7	15.0	18.35	9.30	56	69.97
8	20.0	17.74	9.32	56	65.11
9	25.0	16.73	8.89	59	61.69
10	30.0	13.92	8.57	64	54.87

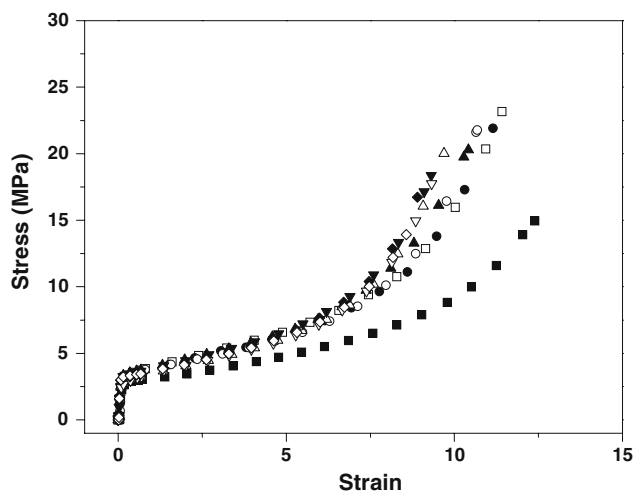


Fig. 2 Stress-strain curves of SEBS-g-MA-silica hybrids with interphase bonding; silica% in matrix: 0 (■), 2.5 (□), 5.0 (●), 7.5 (○), 10.0 (▲), 12.5 (△), 15.0 (▼), 20.0 (▽), 25.0 (◆), 30.0 (◇)

combined with the inorganic network. It is also clear that addition of silica network provided reinforcement to hybrid materials.

The stress-strain data and isotherms for these hybrid materials with 2 to 20-wt.% clay are given in Table 3 and Fig. 3. The maximum value (86 MPa) of modulus integrated from the stress-strain data is noted with 8-wt.% clay contents in the polymer matrix. The maximum stress was found to increase initially with increase in the clay contents, and then at 10-wt.% clay showed a maximum value of 19.5 MPa (relative to the 14.9 MPa of pure copolymer), which represents some improvements in tensile strength. Further addition of clay decreases the strength because of increasing brittleness. The incorporation of clay reinforces the copolymer matrix, depicting the observed increase in the tensile strength as compared to pure copolymer. The length at rupture (maximum extensibility) was found to increase up to 10-wt.% clay and then decreases. The toughness of these hybrids determined from the data show an increase up to 10-wt.% clay, followed by a gradual decrease as can be seen from the results of mechanical properties (Table 3). Maximum interaction between organic and inorganic phases can be achieved when clay layers are fully dispersed homogeneously throughout the matrix. This is possible when the concentration of clay is small, particularly in the present case up to 10-wt.%. When concentration of clay is small the dispersion of individual silicate sheets is at their maximum. When the amount of clay in the polymer matrix increases beyond certain limits, the silicate sheets may exist in the form of the tactoids. This may lead to less cohesion with organic phase

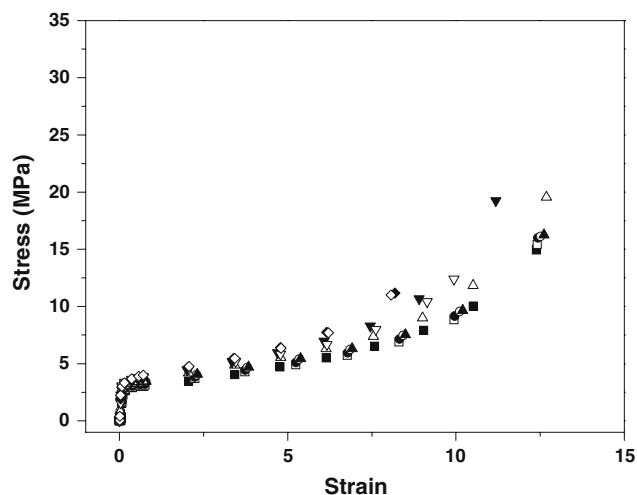


Fig. 3 Stress-strain curves of SEBS-g-MA-clay hybrids; clay% in matrix: 0 (■), 2 (□), 4 (●), 6 (○), 8 (▲), 10 (△), 12 (▼), 14 (▽), 16 (◆), 20 (◇)

causing adverse effects on the mechanical properties. So as the percentage of clay increases the layers may stack together and intergallery space do not increase much so that more chains can travel into space between the layers. These large size particles then degrade the properties of composites.

DMTA measurements

The hybrid films of SEBS-g-MA and silica were subjected for dynamic mechanical thermal measurements and the variation of the loss $\tan \delta$ with temperature for pure SEBS-g-MA and its hybrids with silica are depicted in Fig. 4. These results show that with an increase in temperature, onset of segmental motion starts with a sharp increase in $\tan \delta$ at 88.93 °C. This peak corresponds to the α -relaxation temperature associated with T_g for pure SEBS-g-MA. The sharp peaks for the hybrid materials are observed at slightly higher temperature than those for the pure copolymer and variation in the location of the maxima with silica contents is given in Table 4. The addition of silica shifts the peaks to slightly higher temperatures because the inorganic network hinders segmental motions of the polymer chains. There is a slight displacement of the maxima for 10-wt.% or more silica in the matrix and then becomes constant. At high temperature, loss modulus increases due to alignment of polymer chains with vibration of the sample. The peaks generally decrease in intensity and broaden with increase in the amount of silica.

The temperature variation of storage modulus data is given in Fig. 5. The hybrids give higher modulus than

Table 3 Mechanical Properties of SEBS-g-MA-clay hybrid materials

Sample No.	Clay Contents (%)	Maximum Stress (MPa) ± 3.00	Maximum Strain ± 0.02	Initial Modulus (MPa) ± 0.02	Toughness (MPa) ± 5.00
1	0.0	14.93	12.39	55	79.35
2	2.0	15.42	12.41	56	79.03
3	4.0	15.99	12.43	57	82.09
4	6.0	16.12	12.51	86	85.62
5	8.0	16.25	12.61	86	87.03
6	10.0	19.54	12.68	84	99.04
7	12.0	19.22	11.18	85	87.33
8	14.0	12.38	9.93	64	64.10
9	16.0	11.16	8.18	68	51.58
10	20.0	10.99	8.07	82	50.28

pure SEBS-g-MA elastomer at low temperature due to the introduction of the inorganic component. The increased proportion of silica increases the storage modulus up to a point beyond which the inorganic phase increases the brittleness to the extent of lowering the modulus. Modulus value retained more at high temperature for the sample with silica concentration 20-wt.% and did not fall as steeply as pure copolymer or 5-wt.% silica in the matrix.

DMTA on SEBS-g-MA / clay samples was carried out and temperature dependence loss modulus ($\tan\delta$) for pure elastomer and for hybrids is shown in Fig. 6. The pure elastomer shows a peak at 88.93°C and shift in this value of hybrid materials with different percentages of clay is negligible (Table 5). The shift in the T_g values clearly indicates that clay has poor interaction with copolymer matrix as it has been observed in the mechanical data. The temperature dependence storage modulus is given in Figure 7. The storage moduli of clay hybrids show higher values than pure elastomer at low temperature due to the incorporation

of layered silicates in the matrix. At higher temperature moduli decrease due to the flexibility of the copolymer matrix. The increased amounts of clay increase the storage modulus of the hybrids.

TGA measurements

Thermal stability of SEBS-g-MA-silica ceramers is measured by TGA in temperature range (100–700 °C). The thermograms obtained for hybrid samples under a

Table 4 Glass transition temperatures of SEBS-g-MA silica hybrid materials

Sample No.	Silica Contents (%)	T _g (°C)
1	0.0	88.93
2	5.0	89.25
3	10.0	93.93
4	15.0	93.94
5	20.0	93.82
6	25.0	93.96

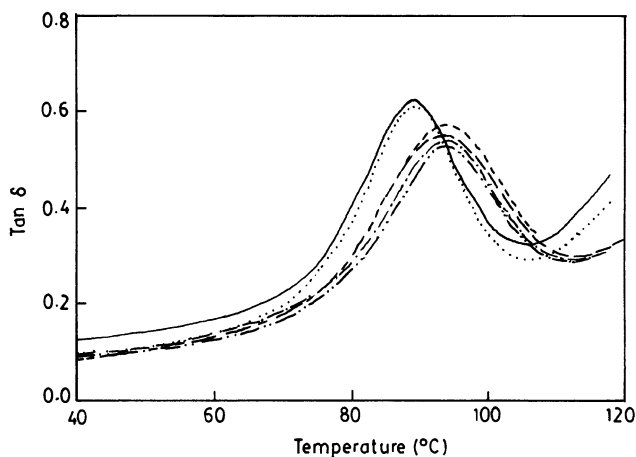


Fig. 4 Variation of loss tangent ($\tan\delta$) with temperature for SEBS-g-MA-silica hybrids at 5 Hz. Wt.% silica in Hybrid: 0 (—), 5.0 (.....), 10.0 (---), 15.0 (— · —), 20.0 (— · — · —), 25.0 (— · — · —)

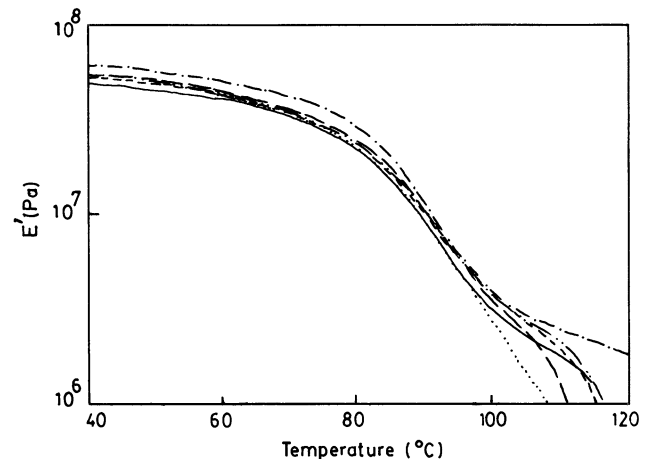


Fig. 5 Temperature dependence of the storage modulus for SEBS-g-MA-silica hybrids at 5 Hz. Wt.% silica in Hybrid: 0 (—), 5.0 (.....), 10.0 (---), 15.0 (— · —), 20.0 (— · — · —), 25.0 (— · — · —)

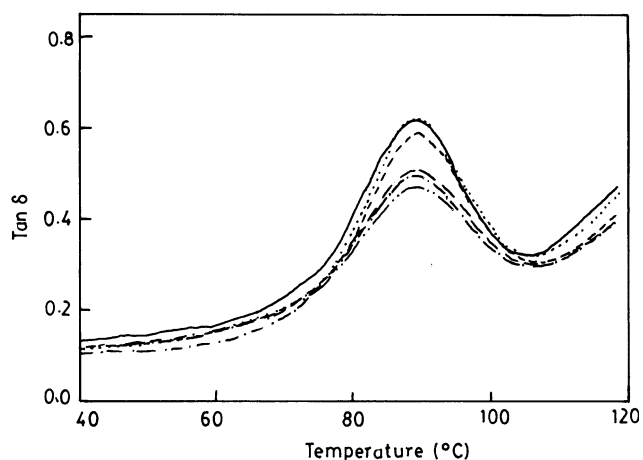


Fig. 6 Variation of loss tangent ($\tan\delta$) with temperature for SEBS-g-MA-clay hybrids at 5 Hz. Wt.% clay in Hybrid: 0 (—), 4 (.....), 8 (---), 12 (----), 16 (-----), 20 (-----)

Table 5 Glass transition temperatures of SEBS-g-MA-clay hybrid materials

Sample No.	Clay Contents(%)	T _g (°C)
1	0	88.93
2	4	89.24
3	8	89.48
4	12	89.50
5	16	89.55
6	20	89.56

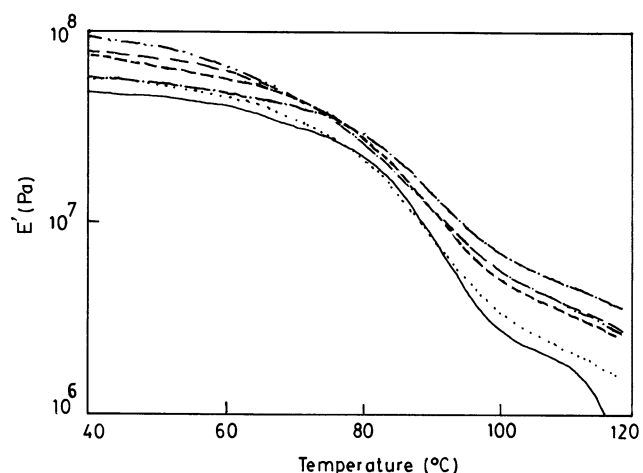


Fig. 7 Temperature dependence of the storage modulus SEBS-g-MA-clay hybrids at 5 Hz. Wt.% clay in Hybrid: 0 (—), 4 (.....), 8 (---), 12 (----), 16 (-----), 20 (-----)

nitrogen atmosphere at a heating rate of 10 °C min⁻¹ are shown in Figure 8. Thermal decomposition temperatures were found in the range of 480–505 °C.

The network structure introduced was expected to increase this temperature. A slight decrease in the rate

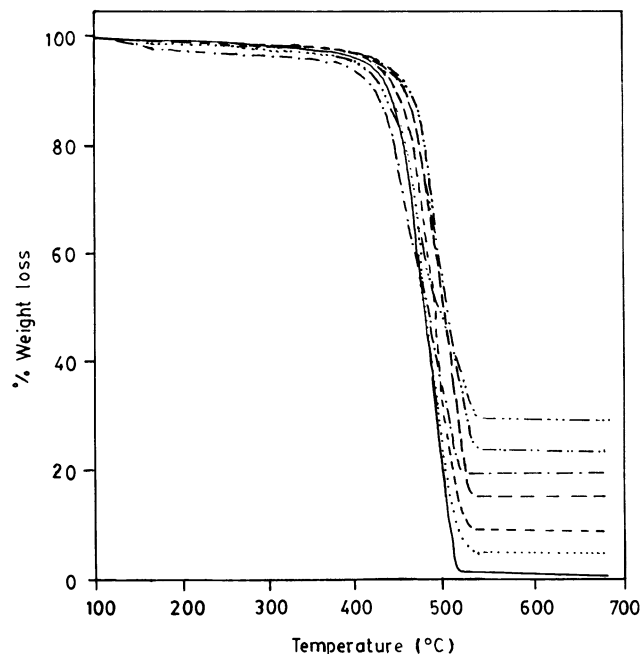


Fig. 8 TGA curves for SEBS-g-MA-silica hybrids with different silica contents obtained at a heating rate of 10°C min⁻¹ in nitrogen; silica% in matrix: 0 (—), 5.0 (.....), 10.0 (---), 15.0 (----), 20.0 (-----), 25.0 (-----), 30.0 (-----)

of weight loss was found with the composites containing large amount of silica because silica network was extensively cross-linked around the polymer chains. The mass of residue retained at 700 °C was found almost proportional to the silica contents in the hybrids. TGA curves carried out under a nitrogen atmosphere for SEBS-g-MA-clay hybrids are shown in Fig. 9. Thermograms for this system were measured in inert atmosphere at a heating rate of 10 °C min⁻¹. The thermal decomposition temperatures of the materials were generally in the range 450–500 °C. TGA results indicate that the pure SEBS-g-MA has a thermal decomposition temperature around 450 °C that increases with addition of clay contents in the copolymer matrix. The weights of residues left after the decomposition at 700°C were found to be approximately proportional to the clay contents in the hybrids.

Conclusions

Organic-inorganic composite materials were prepared by the in-situ generation of inorganic domains through hydrolysis/condensation of TEOS as well as by dispersing the organoclay in the copolymer matrix. The transparency of hybrid materials decreased relative to the pure copolymer in all the systems studied. Improvement in tensile strength was observed in the

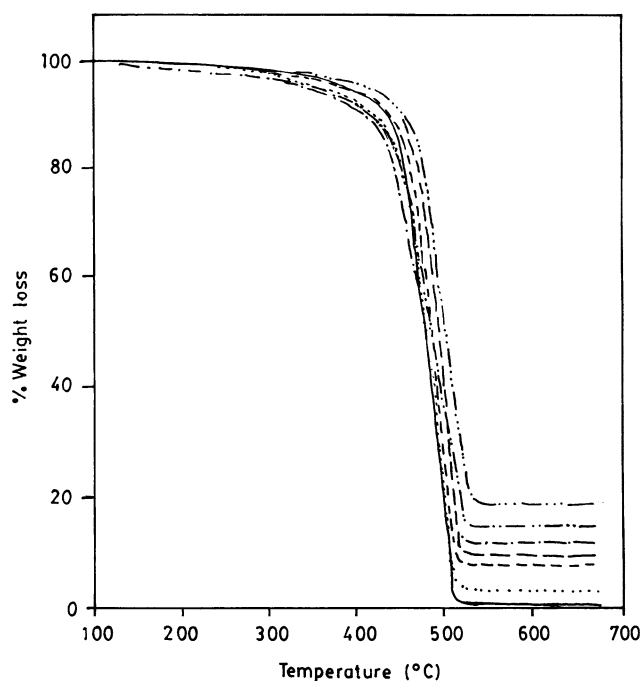


Fig. 9 TGA curves for SEBS-g-MA-clay hybrids with different clay contents obtained at a heating rate of $10^{\circ}\text{C min}^{-1}$ in nitrogen; clay% in matrix: 0 (—), 4 (.....), 8 (---), 10 (----), 12 (-----), 16 (— · — · —), 20 (— · — · —)

copolymer–silica un-compatible and compatibilized systems. The reinforcement in un-compatible system was found to be 50%. However, improvement in compatibilized hybrids is small relative to un-compatible ones. Copolymer–clay composites showed enhancement in the mechanical strength over the pure copolymer as well. The slight shift in T_g maxima upon the addition of silica indicates physical interaction among the phases while in clay hybrids this effect is very less pronounced suggesting poor interaction between the two phases. The thermal stability of the composites increased with the incorporation of the inorganic contents.

References

1. Klein LC (1988) Sol-Gel technology for thin films, performs, electronics and specialty shapes. Noyes, Park Ridge, NJ
2. Mark JE (1989) Chemtech 19:230
3. Brinker CJ, Scherer GW (1990) Sol-Gel science: The physics and chemistry of sol-gel processing. Academic Press, Boston
4. Schmidt H (1990) Better ceramic through chemistry IV. In: Zelinski BJJ, Brinker CJ, Clark DE, Ulrich DR (eds) Mater Res Soc Symp Proc, vol 180, Pittsburg, PA
5. Mark JE (1992) J Appl Polym Sci Appl Polym Symp 50:273
6. Mark JE (1991) J Inorg Orgmet Polym 1:431
7. Schmidt H (1994) J Sol-Gel Sci Tech 1:217
8. Mark JE, Wang S, Ahmad Z (1995) Macromol Symp 98:731
9. Schmidt H (1985) J Non-Cryst Solid 73:681
10. Philipp G, Schmidt H (1984) J Non-Cryst Solids 63:283

11. Schmidt H, Kasemann R, Burkhart T, Wagner G, Arpac E, Geiter E (1995) Hybrid organic-inorganic composites, vol 585. In: Mark JE, Lee CY-C, Bianconi PA (eds) Am Chem Soc, Washington, p 331
12. Yano S, Furukawa T, Kodomari M (1995) High technology composites in modern applications. In: Paipetis S, Youtsos AG (eds) University of Patras, p 46
13. Sur GS, Mark JE (1985) Eur Polym J 21(2):1051
14. Huang HH, Oler B, Wilkes GL (1987) Macromolecules 20:1322
15. Wang B, Wilkes GL (1991) J Polym Sci Part A: Polym Chem Ed 29:905
16. Brennan AB, Rodrigues DE, Wang B, Wilkes GL (1992) In: Hench LL, West JK (eds) Chemical processing of advanced materials. Wiley, New York
17. Betrabet CS, Wilkes GL (1995) Chem Mater 7:535
18. Ahmad Z, Wang S and Mark JE (1995) Hybrid organic-inorganic composites, vol. 585. In: Mark JE, Lee CY-C, Bianconi PA (eds) Am Chem Soc, Washington, p 291
19. Wang S, Ahmad Z, Mark JE (1994) Chem Mater 6:943
20. Wang S, Ahmad Z, Mark JE (1994) Macromol Reports A31:411
21. Ahmad Z, Sarwar MI, Mark JE (1997) J Mater Chem 7:259
22. Ahmad Z, Sarwar MI, Wang S, Mark JE (1997) Polymer 38:4523
23. Rehman HU, Sarwar MI, Ahmad Z, Krug H, Schmidt H (1997) J Non-Cryst Solids 211:105
24. Ahmad Z, Sarwar MI, Krug H, Schmidt H (1997) Die Angew Makromol Chem 248:139
25. Ahmad Z, Sarwar MI, Mark JE (1997) J Appl Polym Sci 63:1345
26. Ahmad Z, Sarwar MI, Mark JE (1998) J Appl Polym Sci 70:297
27. Okada A, Kawasumi M, Usuki A, Kojimi Y, Kurauchi T, Kamigato O (1990) Mater Res Symp Proc 171:45
28. Gianellis EP (1996) Adv Mater 8:29
29. Zilg C, Mulhaupt R, Finter J (1999) Macromol Chem Phys 200(3):661
30. Ke Y, Lu J, Yi X, Zhao J, Qi Z (2000) J Appl Polym Sci 78:808
31. Kornmann X, Lindberg H, Berglund LA (2001) Polymer 42:4493
32. Sikka M, Cerini LN, Ghosh SS, Winey KI (1996) J Polym Sci Part B Polym Phys 34:1443
33. Vaia RA, Jandt KS, Kramer EJ, Gianellis EP (1995) Macromolecules 28:8080
34. Gilman JW, Jackson CL, Morgan AB, Harris R (2000) J Chem Mater 12:1866
35. Fu X, Qutubuddin S (2001) Polymer 42:807
36. Park CI, Park OO, Lim JG, Kim HJ (2001) Polymer 42:7465
37. Lee DC, Jang LW (1996) J Appl Polym Sci 61:1117
38. Kato M, Usuki A, Okada A (1997) J Appl Polym Sci 66:1781
39. Manias E, Touny A, Wu L, Lu B, Strawhecker K, Gilman JW, Chung TC (2000) Polym Mater Sci Eng 82:282
40. Ke Y, Long C, Qi Z (1999) J Appl Polym Sci 71:1139
41. Huang JC, Zhu ZK, Yin J, Qian XF, Sun YY (2001) Polymer 42:873
42. Chen Z, Huang C, Liu S, Zhang Y, Gong K (2000) J Appl Polym Sci 75:796
43. Agag T, Koga T, Takeichi T (2001) Polymer 42:3399
44. Tyan HL, Liu YC, Wei KH (1999) Chem Mater 11:1942
45. Manias E, Zax DB, Anastasiadis SH (2000) Polym Mater Sci Eng 82:259
46. Vaia RA, Gianellis EP (2001) Polymer 42:1281
47. Gloagen JM, Lefebvre JM (2001) Polymer 42:5841
48. Brennan AB, Wilkes GL (1991) Polymer 32:733